Analysis of the intensity photometric of comet inner coma

Ruaa J. Oheeb[1] and *Salman* Z. Khalaf[1*]

[1]Department of Astronomy and Space, College of Science, University of Baghdad, Baghdad, Iraq

Abstract. In this research, image of comet Leonard (C/2021 A1 Leonard), Hale-Bopp (C/1995 O1 Hale-Bopp), (C/2020 F3 NEOWISE) and (C/2006 P1 McNaught) were studied and analyzed for the purpose of studying the distribution of light intensity across the primary colors (red, green, blue) to understand the physical characteristics of light intensity with distance using the MATLAB program. And to find the relationship of each comet and how to change the behavior of the light intensity of these comets, as the results showed a good relationship to the distribution of intensity and how the change occurs in the brightness of each comet. As a result, we notice that as the distance increases, the brightness gradually increases, and the relationship is direct, but at values ranging from (100-150), the intensity begins to decrease gradually as the distance increases. As a comet approaches the Sun, the icy material in its nucleus begins to sublimate, releasing complex organic molecules into the coma. These protomolecules were tracked using infrared and radio wave detection techniques.

1 Introduction

The solar wind directly affects the formation of a comet's tail [1]. When a comet approaches the sun, the icy nucleus releases gases that are ionized by ultraviolet radiation [2, 3]. The solar wind pushes the ions away from the comet, in the opposite direction to the sun, forming a long ion tail [4, 5]. Therefore, it can be used to monitor the speed and direction of the solar wind [6, 7]. When solar storms occur, the ions accelerate, forming a large ion halo around the nucleus due to the expansion of the plasma region surrounding the comet [8, 9]. Comets have two types of tails: a dust tail made up of dust particles, and an ion tail made up of ionized gases emitted from the nucleus [10]. In recent decades, there has been increasing interest in observing comets and studying the interactions of comet tails with the solar wind [11, 12], most notably comets Leonard (C/2021 A1 Leonard)[13], Hale-Bopp (C/1995 O1 Hale-Bopp) [14], (C/2020 F3 NEOWISE) and (C/2006 P1 McNaught). In 2008, Salman Z. Khalaf demonstrated in his research the study of the interaction between the solar wind and comet tail ions in the present-day atmosphere through MHD studies. This was achieved using an explicit Lachs-Wendorff simulation model for three-dimensional space [3]. Comet Leonard was discovered and reached perihelion in 2022, so it was observed by several telescopes such as Hubble and Gemini North. During the observation, a rapid development in the comet's ion

* Corresponding author: salman.zkhalaf72@gmail.com

tail was revealed. A spectroscopic analysis study also showed the possibility of the comet's nucleus undergoing partial disintegration during the period of proximity to the Sun. As for Comet Hale-Bopp, it was discovered in 1995 and reached perihelion in 1997. Its brightness and the long period characterize it, making it visible to the naked eye. It was observed by several telescopes such as Hubble and ALMA. Through observation, it was found that its atmosphere contains a number of molecular compounds such as HCN, CH3OH, and H2CO. These studies provided explanations for understanding the physics of comets by analyzing models based on accurate physical equations [15].

Fig. 1. Represents Comet Hale-Bopp.

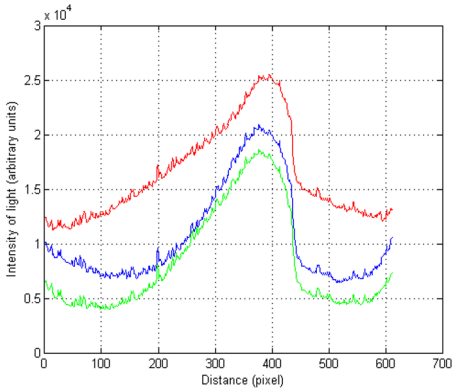

Fig. 2. Relation between light intensity (arbitrary unit) and distance (pixel) for comet Hale-Bopp.

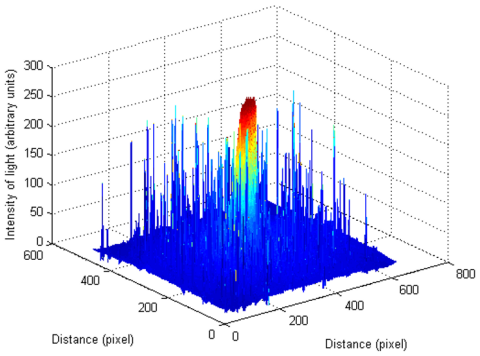

Fig. 3. Light intensity changes with distance, three dimensions for the red color comet Hale-Bopp.

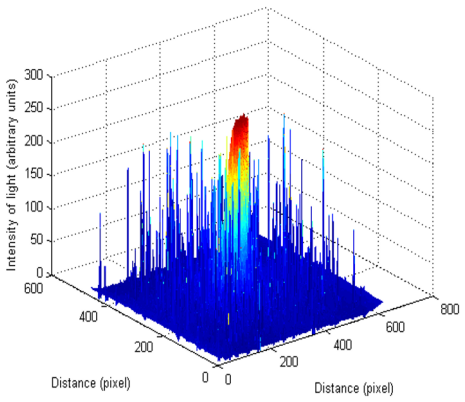

Fig. 4. Light intensity changes with distance, three dimensions for the green color comet Hale-Bopp.

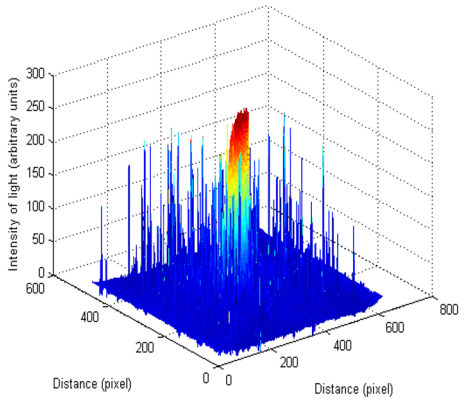

Fig. 5. Light intensity changes with distance, three dimensions for the blue color comet Hale-Bopp.

Fig. 6. Represent the Leonard comet through interaction between solar wind and coma.

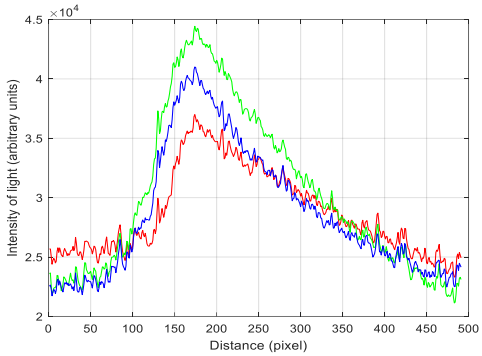

Fig. 7. Relation between light intensity (arbitrary unit) and distance (pixel) for comet Leonard.

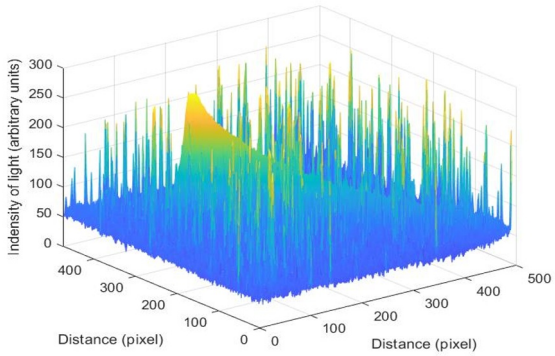

Fig 8. Light intensity changes with distance, three dimensions for red color comet Leonard.

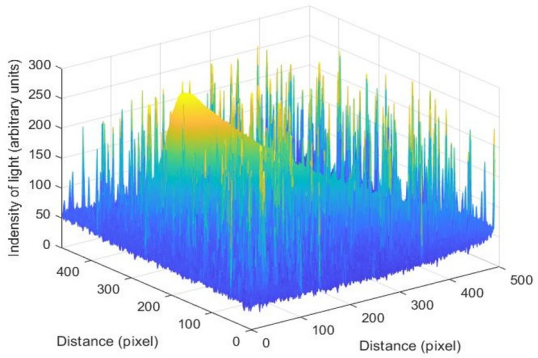

Fig. 9. Light intensity changes with distance, three dimensions for green color comet Leonard

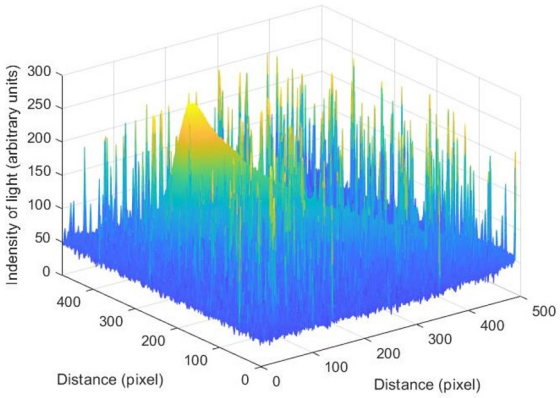

Fig. 10. Light intensity changes with distance,three dimensions for blue color comet Leonard

Fig. 11. Represents Comet McNaught.

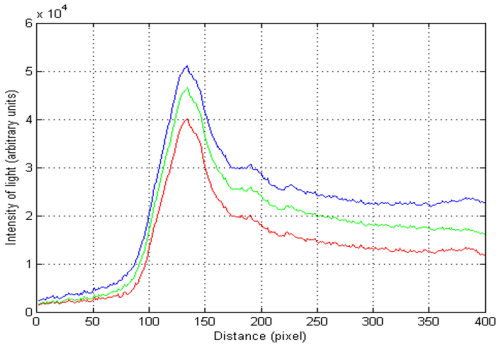

Fig. 12. Relation between light intensity (arbitrary unit) and distance (pixel) for comet McNaught.

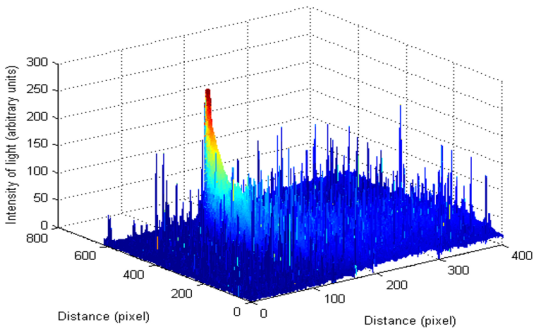

Fig. 13. Light intensity changes with distance, three dimensions for red color comet McNaught.

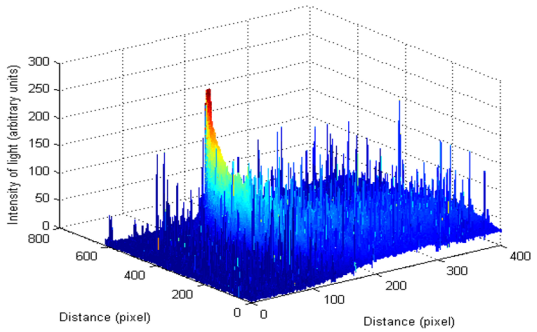

Fig. 14. Light intensity changes with distance, three dimensions for green color comet McNaught.

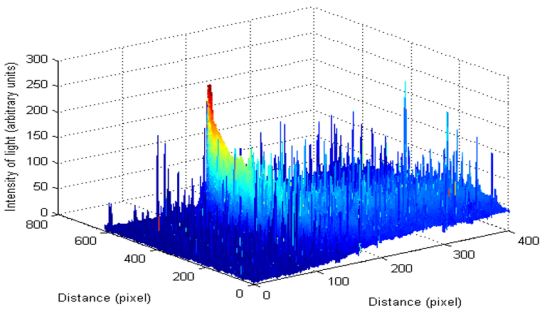

Fig. 15. Light intensity changes with distance, three dimensions for blue color comet McNaught.

Fig. 16. Represents Comet NEOWISE.

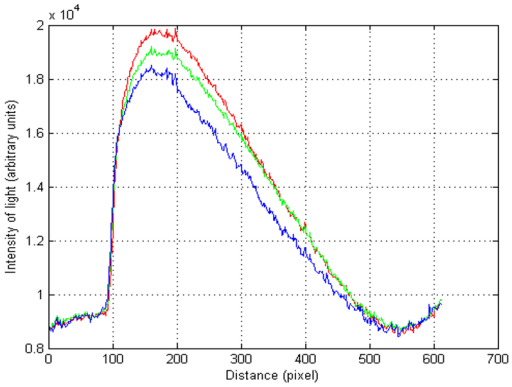

Fig. 17. Relation between light intensity (arbitrary unit) and distance (pixel) for comet NEOWISE.

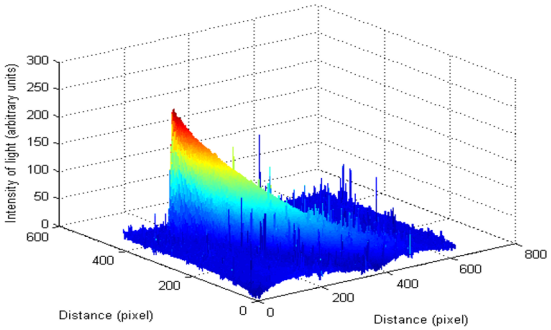

Fig. 18. Light intensity changes with distance, three dimensions for red color comet NEOWISE.

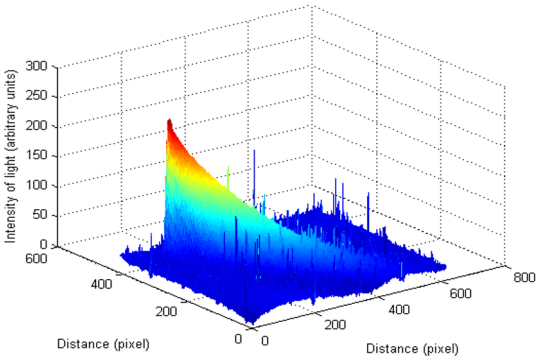

Fig. 19. Light intensity changes with distance, three dimensions for green color comet NEOWISE.

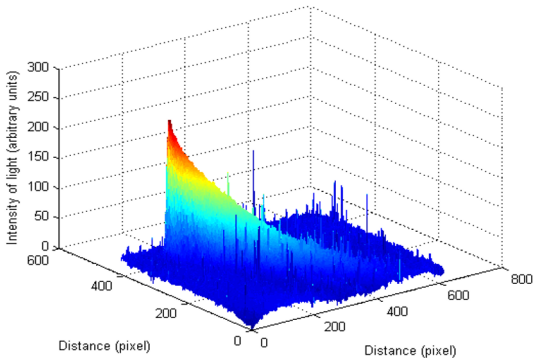

Fig. 20. Light intensity changes with distance, three dimensions for blue color comet NEOWISE.

2 Image-based intensity analysis

Optical images of comets Hale-Bopp, Leonard, Neweys, and McNaught represent color intensity in the RGB color channel. Figures (2, 7, 12, 17) for the comets show the exact distribution of color brightness. In Hale-Bopp, red is the most intense, followed by green and then blue. This indicates high energy and temperature in the nucleus, as well as being extremely bright. Brightness is highest near the center of the comet and decreases toward the tail. Figures (3, 4, 5) represent the RGB color distribution in the center, indicating a concentration of thermal and radioactive activity in the nucleus. For Comet Leonard, the data show that the optical properties are different. In Figure 7, the green channel has the highest intensity, followed by red and blue. This also indicates that the nucleus' brightness is less intense and more diffused compared to Hale-Bopp. The intensity distribution in Figures (8, 9, 10) shows a broad peak, indicating that the energy emission in this comet is more diffuse. While Comet McNaught, as shown in Figures (13, 14, 15) shows high radiation at the nucleus, and the color intensity indicates a large scattering of reflective particles, Comet NEOWISE, as shown in Figures (18, 19, 20) shows the highest intensity for positive red wavelengths, meaning that the temperature of this region is lower because it emits a red spectrum.

3 Mathematical representation of heat distribution

According to the Stefan-Boltzmann law, the intensity of any optical image is related to temperature.

$$F=\sigma T^4 \quad (1)$$

where F is a flux in unit watts/m2and σ is Steven Boltzmann constant.
The total luminosity from an object would be

$$L=4\pi R^2 \sigma T^4 \quad (2)$$

By analyzing comet images, it was shown that the thermal distribution reflects how energy is distributed within the comet and shows the extent of the nucleus' activity and the sites of evaporation. It was also shown that the temperature around the nucleus indicates the comet's activity.

$$TD = e^{0.0143*d} \quad (3)$$

d represents the distance from the tail to the nucleus. The values of d differ for comets, with the highest value being for Hale-Bopp's comet (0<d<396), Leonard's comet (0<d<174), Newways comet (0<d<195), and McNutt's comet (0<d<200) .

$$TD=255/e^{0.03(d-p)} \quad (4)$$

This model was applied to the four comets based on analytical images in which the point representing the nucleus (peak intensity (P)) was identified and the thermal pattern passing through it was extracted. The results revealed clear differences that reflect the physical and astronomical properties of each comet.

Table 1. The peak intensities for comets Hale-Bopp, Leonard, Newise, and McNaught

The Comet	Peak intensity(P)
Hale-Bopp	396
Leonard	174
NEOWISE	195
McNaught	200

The highest value was for comet Hale-Bopp and the lowest for comet Leonard.
For Hale-Bopp, the exponential decay function used after the nucleus using Equation (4) reveals numerous differences in the compositional and thermal structures of the comets. Hale-Bopp exhibited a highly extended thermal structure and a gradual decrease in temperature, indicating a large, active nucleus and a long tail. McNaught and Leonard, on the other hand, had a higher thermal gradient, showing less thermal activity and shorter tails. Although McNaught and NEOWISE had similarities, NEOWISE exhibited a higher thermal activity. Although the same equation was applied to all comets, the differences between them provide a quantitative indicator of the differences in shape, energy, and structure of these celestial bodies.

By analyzing the colors of comets and converting them to wavelengths corresponding to RGB colors using Wien's shift law in equation (5), the temperatures of different regions of the comet can be estimated, in addition to analyzing the change in temperatures according to the difference in the color of radiation. as follows:

$$\lambda max\ T = 2.898X10\text{-}3\ k \quad (5)$$

The equation was applied to the following wavelengths using Wien's displacement law, we calculated the color temperatures of red, green and blue:

Table 2. The temperatures of green, red, and blue light based on the wavelengths of the comets.

Colors	The wavelengths(λ)nm	Temperatures(K)
Red	700	4140
Green	560	5175
Blue	490	5914

By applying equation (5), it is clear that the closer the color is to blue, the higher the temperature, and this indicates that the gas or dust emitted from it is very hot. However, if it is reddish, its temperature is lower, and this is consistent with the physics of radiation for hot bodies.

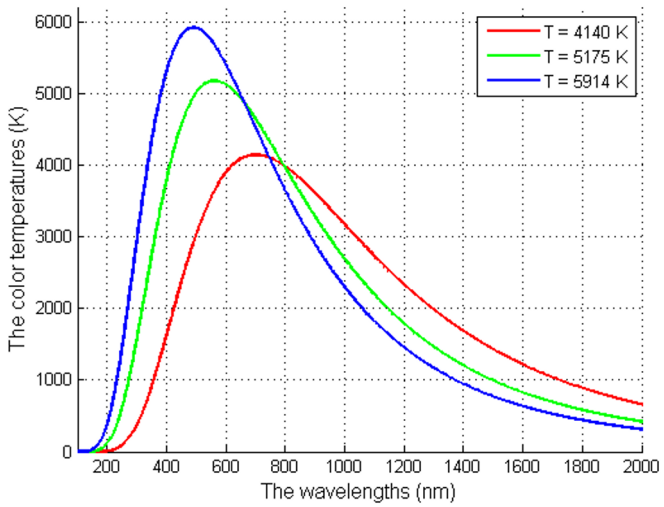

Fig. 21. Wavelengths of RGB colors emitted by comets and their relationship to temperature.

This figure shows the distribution of radiation intensity as a function of wavelength for red, green, and blue, which is related to the color temperature of comets. The three curves (red, green, and blue) represent the radiation behavior of comets at different temperatures.

4 Conclusions

1. The analysis results show that the comet image can be divided into four distinct regions, characterized by optical clarity and specific properties. These regions include the

background, the tail-wasting region, the nucleus, and the surrounding region. Each region exhibits clear distinctions in terms of optical density and optical structure.
2. The distribution of light intensity in the comet follows a mathematical pattern that can be described by two equations that vary depending on the relative position of the point from the center of the nucleus. It was found that the light intensity gradually increases according to a smooth positive exponential function extending from the beginning of the tail to the center of the nucleus, while it decreases sharply after passing the center, according to a negative exponential function until the end of the comet.
3. The directions of the light intensity flow, as represented by illustrative arrows, indicate that the flow movement is clearly directed toward the center of the nucleus, reflecting an organized optical behavior that supports the hypothesis of a concentration of activity in the central region.
4- The optical density shows a significant decrease with increasing distance from the nucleus. This decrease is attributed to the influence of both magnetic pressure and solar wind, as the two factors interact within a dynamic framework that affects the behavior of plasma particles within the environment surrounding the comet.

References

1. F. Moreno, C. Goetz, F.J. Aceituno, V. Casanova, A. Sota, P. Santos-Sanz, Dust environment of long-period comet C/2023 A3 (Tsuchinshan-ATLAS). Monthly Notices of the Royal Astronomical Society **539**, 2, 949-955 (2025) https://doi.org/10.1093/mnras/staf552
2. E. Mozhenkov, O. Vaisberg, On the classification of comet plasma tails. Solar System Research **51**, 258-270 (2017) https://doi.org/10.1134/S0038094617040037
3. E. Bonamente, D.J. Christian, Z. Xing, K. Venkataramani, D. Koutroumpa, et al, Variable X-Ray Emission of Comet 46P/Wirtanen. The Planetary Science Journal, **2**(6), 224, (2021) https://doi.org/ff10.3847/psj/ac2aac
4. D. Bockelée-Morvan, U. Calmonte, S.B. Charnley, J. Duprat, C. Engrand, et al, Cometary Isotopic Measurements. Space Science Reviews, **197**(1-4), 47-83 (2015). https://doi.org/ff10.1007/s11214-015-0156-9
5. S.R. Watson, C.J. Scott, M.J. Owens, L.A. Barnard, Solar wind interactions with comet C/2021 A1 Using STEREO HI and a data-assimilative solar wind model. The Astrophysical Journal **970**, 2, 101 (2024) http://doi.org/10.3847/1538-4357/ad50cf
6. K.-H. Glassmeier, Interaction of the solar wind with comets: a Rosetta perspective. Philosophical Transactions of the Royal Society A: Mathematical, Physical and Engineering Sciences **375**, 2097, 20160256 (2017) https://doi.org/10.1098/rsta.2016.0256
7. S.R. Grant, G.H. Jones, Prospects for the Crossing by Earth of Comet C/2023 A3 Tsuchinshan-ATLAS's Ion Tail. Research Notes of the AAS **8**, 10, 252 (2024) http://doi.org/10.3847/2515-5172/ad83bf
8. D.B. Alexashov, V.B. Baranov, M.G. Lebedev, Three-dimensional magnetohydrodynamic model of the interaction between the solar wind and cometary atmospheres. Fluid Dyn. **50**, 98 (2015). https://doi.org/10.1134/S0015462815010111
9. G. Leone, H.K.M. Tanaka, Igneous processes in the small bodies of the Solar System I. Asteroids and comets. iScience **26**(7), 107160 (2023). https://doi.org/ 10.1016/j.isci.2023

10. N. Biver, et al., Chemical composition of comets C/2021 A1 (Leonard) and C/2022 E3 (ZTF) from radio spectroscopy and the abundance of HCOOH and HNCO in comets. Astronomy & Astrophysics **690**, A271 (2024) https://doi.org/10.1051/0004-6361/202450921
11. D.G. Schleicher, P.V. Birch, T.L. Farnham, A N. Bair, The Extreme Activity in Comet Hale–Bopp (C/1995 O1): Investigations of Extensive Narrowband Photoelectric Photometry. The Planetary Science Journal **5**, 12, 281 (2024) https://doi.org/10.3847/PSJ/ad86b9
12. Ch. Götz, J. Deca, K. Mandt, M. Volwerk, Solar wind interaction with a comet: evolution, variability, and implication. arXiv:2211.04887, https://doi.org/10.48550/arXiv.2211.04887
13. S. Faggi, M. Lippi, M.J. Mumma, G.L. Villanueva, Strongly depleted methanol and hypervolatiles in comet C/2021 A1 (Leonard): signatures of interstellar chemistry? The Planetary Science Journal **4**, 1, 8 (2023) https://doi.org/10.3847/PSJ/aca64c
14. D. Jewitt, Y. Kim, M. Mattiazzo, M. Mutchler, J. Li, J. Agarwal, Disintegration of Long-period Comet C/2021 A1 (Leonard). The Astronomical Journal **165**, 3, 122 (2023) https://doi.org/10.3847/1538-3881/acb53b
15. E.R. Willis, D.A. Christianson, R.T. Garrod, Ice chemistry modeling of active phase comets: Hale–Bopp. Icarus **416**, 116097 (2024) https://doi.org/10.48550/arXiv.2408.15509